

Magnetic and Electronic Properties of $\text{Ru}_{1-y}\text{M}_y\text{Sr}_2\text{Eu}_{2-x}\text{Ce}_x\text{Cu}_2\text{O}_{10+\delta}$ ($\text{M} = \text{Nb}, \text{Sn}$)

S. K. Goh ^{a,b}, E. K. Hemery ^{a,b}, G. V. M. Williams ^a, and H. K. Lee ^c

^a*MacDiarmid Institute for Advanced Materials and Nanotechnology, Industrial Research, P.O. Box 31310, Lower Hutt, New Zealand.*

^b*School of Chemical and Physical Sciences, Victoria University, Private Bag, Wellington, New Zealand.*

^c*Department of Physics, Kwangwon National University, Chunchon, 200-700, Korea and Korea Basic Science Institute, Chunchon Center, Chunchon, 200-701, Korea.*

Partial Sn substitution for Ru in the superconducting and magnetically ordered compound, $\text{RuSr}_2\text{Eu}_{1.2}\text{Ce}_{0.8}\text{Cu}_2\text{O}_{10+\delta}$, leads to a suppression of the magnetic order and an increase in the temperature where the Meissner state commences. This is consistent with the spontaneous vortex phase model. Magnetization measurements on magnetically ordered but not superconducting $\text{RuSr}_2\text{EuCeCu}_2\text{O}_{10+\delta}$ are interpreted in terms of low temperature ferrimagnetic order.

1. Introduction

The ruthenate-cuprates, $\text{RuSr}_2\text{RCu}_2\text{O}_8$ and $\text{RuSr}_2\text{R}_{2-x}\text{Ce}_x\text{Cu}_2\text{O}_{10+\delta}$ ($\text{R}=\text{Eu},\text{Gd},\text{Y}$) are interesting compounds containing 2D CuO_2 and RuO_2 layers. They also exhibit superconductivity and magnetic order. It has been argued that superconductivity and magnetic order can coexist via the formation of a spontaneous vortex phase [1]. In this model, the Meissner state commences at a temperature T_{Meissner} that is lower than the superconducting transition temperature T_c . T_{Meissner} is defined as the temperature where the lower critical field becomes equal to the internal field from the ferromagnetic component of the magnetically ordered Ru moments. It is now generally agreed that the low-field magnetic order in $\text{RuSr}_2\text{RCu}_2\text{O}_8$ is antiferromagnetic with spin-canting [2,3] and there is a field induced spin-flop transition to a ferromagnetic state [4]. The situation in the case of $\text{RuSr}_2\text{R}_{2-x}\text{Ce}_x\text{Cu}_2\text{O}_{10+\delta}$ is not so clear. It has been suggested that the low field magnetic state is antiferromagnetic [5].

2. Experimental details

The preparation of the $\text{Ru}_{1-y}(\text{Sn},\text{Nb})_y\text{Sr}_2\text{Eu}_{2-x}\text{Ce}_x\text{Cu}_2\text{O}_{10+\delta}$ is described elsewhere [6]. X-ray diffraction measurements showed that the samples were single phase. Resistivity measurements were made using the standard four terminal method and room temperature thermopower measurements were made using the standard differential temperature method. Dc and ac magnetization measurements were made using a SQUID magnetometer. The ac measurements were done with an ac magnetic field of 5 μT and at 333 Hz.

3. Results

The ac susceptibility data are plotted in Fig.1 for $\text{RuSr}_2\text{Eu}_{1.2}\text{Ce}_{0.8}\text{Cu}_2\text{O}_{10+\delta}$ and when 0.2 Sn has been substituted for Ru. The large peak ~ 80 K in the pure sample arises from the ferromagnetic component of the magnetic order. There is a gradual decrease in χ' with decreasing temperature. A change in slope occurs at $T_c \sim 31$ K that signals the onset of superconductivity. The entrance into the Meissner state starts at ~ 12 K where χ' becomes

negative. For the 0.2 Sn sample, the large positive χ' has disappeared and it is consistent with the complete suppression of the magnetic order. T_{Meissner} is now ~ 31 K which is close to T_c . Thus, T_{Meissner} is only significantly below T_c when there is magnetic order arising from the RuO_2 planes. This is consistent with the spontaneous vortex phase model [1].

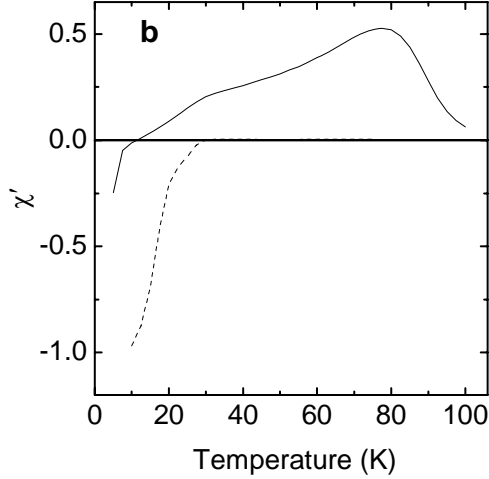


Fig. 1. Plot of the ac susceptibility against temperature for $\text{Ru}_{1-y}\text{Sn}_y\text{Sr}_2\text{Eu}_{1.2}\text{Ce}_{0.8}\text{Cu}_2\text{O}_{10+\delta}$ with $y=0$ (solid curve) and $y=0.2$ (dashed curve).

We now consider non-superconducting $\text{RuSr}_2\text{EuCeCu}_2\text{O}_{10+\delta}$ where the magnetic behaviour is not complicated by the appearance of superconductivity. The resistivity data are plotted in Fig.2 for $\text{Ru}_{1-y}(\text{Sn},\text{Nb})_y\text{Sr}_2\text{Cu}_2\text{O}_{10+\delta}$. Below 100 K all the samples follow a nearly power law dependence and with an exponent ranging from -0.8 to -1.1. The variation in the absolute resistivity values is likely to be due to changes in the hole concentration in the CuO_2 planes. This can be seen in the inset to Fig.2 where the resistivity at 20 K is plotted against the room temperature thermopower, $S(300\text{K})$. For the superconducting cuprates, $S(300\text{K})$ has been found to correlate with the number of doped holes per Cu, p , in the CuO_2 plane, where high $S(300\text{K})$ corresponds to low p [7]. Thus, the data in the inset can be interpreted in terms of the conductivity being dominated by transport in the CuO_2 planes and the variation in the absolute resistivities is due to changes in p possibly arising from different δ values.

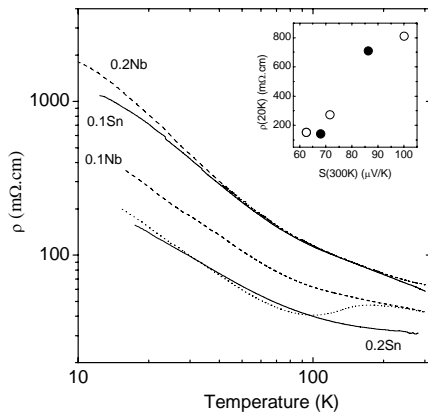


Fig. 2. Plot of the resistivity against temperature for $\text{Ru}_{1-y}\text{Sn}_y\text{Sr}_2\text{EuCeCu}_2\text{O}_{10+\delta}$ with $y=0$ (dotted curve), $y=0.1$ (solid curve) and $y=0.2$ (solid curve). Also shown is data for $\text{Ru}_{1-y}\text{Nb}_y\text{Sr}_2\text{EuCeCu}_2\text{O}_{10+\delta}$ with $y=0.1$ (dash curve) and $y=0.2$ (dash curve). Inset: Plot of the room temperature thermopower against the resistivity at 20 K for the Sn substituted samples (filled circles) and Nb substituted samples (open circles).

The low temperature magnetization data for some of the $\text{Ru}_{1-y}(\text{Sn},\text{Nb})_y\text{Sr}_2\text{Eu}_{2-x}\text{Ce}_x\text{Cu}_2\text{O}_{10+\delta}$ samples are plotted in Fig.3. The rapid saturation of the magnetization with increasing magnetic field and the magnetization values imply a large ferromagnetic component. The

magnetic ordering temperature was estimated from the maximum slope of the temperature dependent magnetization. Typical data for the pure compound are shown in the lower left inset. We find that the magnetic ordering temperature, T_M and the saturation magnetization, M_s , both decrease with increasing Sn or Nb concentrations. Here, M_s , was estimated by extrapolating the high field data in Fig.3 to zero field. It can be seen in the upper right inset to Fig.3 that M_s falls on a common curve when plotted against T_M .

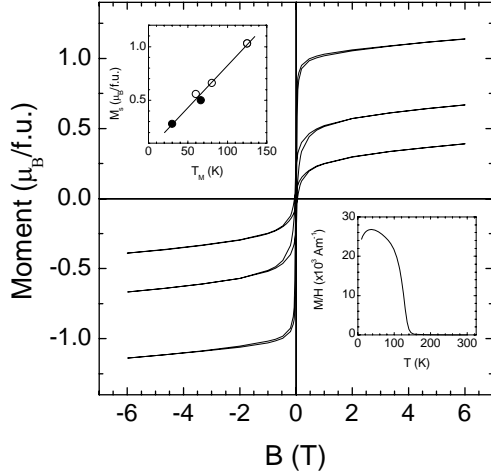


Fig. 3. Plot of the moment per formula unit (f.u.) against the applied field for $\text{Ru}_{1-y}(\text{Sn,Nb})_y\text{Sr}_2\text{Eu}_{2-x}\text{Ce}_x\text{Cu}_2\text{O}_{10+\delta}$. Upper left inset: Plot of the saturation moment per f.u. against the magnetic ordering temperature for Sn (filled circles) and Nb (open circles). Lower right inset: Plot of the zero-field-cooled magnetization from the pure sample with an applied magnetic field of 25 mT.

Magnetization measurements have been made in the Curie-Weiss region (>190 K) and to 400 K to estimate the effective moment and develop a possible model for the magnetic order. We find that the effective moment is $3.10 \pm 0.15 \mu_B/\text{Ru}$ and it does not change with increasing Sn concentration within the experimental uncertainty. Since Ru has a 5+ valence [8], it is possible that the measured effective moment arises from $\sim 45\%$ low spin Ru^{5+} ($S=1/2$) and $\sim 55\%$ high spin Ru^{5+} ($S=3/2$). If the low temperature magnetic order is ferrimagnetic with the moments of high spin Ru^{5+} aligned antiparallel to that of low spin Ru^{5+} , then this mixture of high and low spin electronic configurations can lead to a net measured low temperature moment of $\sim 1.2 \mu_B/\text{Ru}$, which is close to that obtained from the magnetization data ($1.07 \mu_B/\text{Ru}$).

Acknowledgments

We acknowledge funding support by the New Zealand Marsden Fund, the Alexander von Humboldt Foundation (GVMW), Industrial Research Limited (SKG) and the MacDiarmid Institute for Advanced Materials and Nanotechnology (EKH). We also thank Jeff Tallon and Neil Ashcroft for useful comments.

References

- [1] E. B. Sonin and I. Felner, Phys. Rev. B **57**, 14000 (1998).
- [2] J. W. Lynn, B. Keimer, C. Ulrich, C. Bernhard, and J. L. Tallon, Phys. Rev. B **61**, 14964 (2000).
- [3] J. D. Jorgensen, O. Chmaissem, H. Shaked, S. Short, P. W. Klamut, B. Dabrowski, and J. L. Tallon, Phys. Rev. B **63**, 54440 (2001).
- [4] G. V. M. Williams and S. Krämer, Phys. Rev. B **62**, 4132 (2000).
- [5] I. Felner, U. Asaf, and O. Millo, Phys. Rev. B **55**, 3374 (1997).
- [6] G. V. M. Williams and M. Ryan, Phys. Rev. B **64**, 94515 (2001).
- [7] J. L. Tallon, C. Bernhard, R. L. Hitterman, and J. D. Jorgensen, Phys. Rev. B **51**, 12911 (1995).
- [8] G. V. M. Williams, L. Y. Jang, and R. S. Liu, Phys. Rev. B **65**, 64508 (2002).